

## ON THE SOLAR NICKEL AND OXYGEN ABUNDANCES

PAT SCOTT,<sup>1,2,4</sup> MARTIN ASPLUND,<sup>3,4</sup> NICOLAS GREVESSE<sup>5,6</sup> AND A. JACQUES SAUVAL<sup>7</sup>*Submitted to ApJL*

## ABSTRACT

Determinations of the solar oxygen content relying on the neutral forbidden transition at 630 nm depend upon the nickel abundance, due to a Ni I blend. Here we rederive the solar nickel abundance, using the same *ab initio* 3D hydrodynamic model of the solar photosphere employed in the recent revision of the abundances of C, N, O and other elements. Using 17 weak, unblended lines of Ni I together with the most accurate atomic and observational data available we find  $\log \epsilon_{\text{Ni}} = 6.17 \pm 0.05$ , a downwards shift of 0.06–0.08 dex relative to previous 1D-based abundances. We investigate the implications of the new nickel abundance for studies of the solar oxygen abundance based on the [O I] 630 nm line in the quiet Sun. Furthermore, we demonstrate that the oxygen abundance implied by the recent sunspot spectropolarimetric study of Centeno & Socas-Navarro needs to be revised downwards from  $\log \epsilon_{\text{O}} = 8.86 \pm 0.07$  to  $8.71 \pm 0.10$ . Determinations of the solar oxygen content relying on forbidden lines now appear to converge around  $\log \epsilon_{\text{O}} = 8.7$ .

*Subject headings:* line: formation — line: profiles — Sun: abundances — Sun: atmosphere — Sun: photosphere — techniques: polarimetric

## 1. INTRODUCTION

The reference solar oxygen abundance has been revised over the past decade from  $\log \epsilon_{\text{O}} = 8.93 \pm 0.04$  (Anders & Grevesse 1989) via  $8.83 \pm 0.06$  (Grevesse & Sauval 1998, GS98) to  $8.66 \pm 0.05$  (Asplund et al. 2005, AGS05). This downward slide has been brought on by the tandem influences of three-dimensional photospheric models, treatment of departures from local thermodynamic equilibrium (LTE), identification of blends, improved atomic data and better observations (Allende Prieto et al. 2001; Asplund et al. 2004). The new abundances of oxygen and other elements have solved many outstanding problems, but ruined agreement between helioseismological theory and observation (see e.g. Basu & Antia 2008). This has prompted a reanalysis of photospheric models, resulting in support for high (Ayres et al. 2006; Centeno & Socas-Navarro 2008; Ayres 2008), low (Scott et al. 2006; Socas-Navarro & Norton 2007; Koesterke et al. 2008; Meléndez & Asplund 2008) and intermediate (Caffau et al. 2008) solar oxygen abundances.

Many of these analyses rely upon the forbidden oxygen line at 630 nm, known to contain a significant blend from Ni I. The strength of this blend, and therefore the  $\epsilon_{\text{O}}$  indicated by [O I] 630 nm, depend critically upon the solar nickel abundance ( $\epsilon_{\text{Ni}}$ ). This is no less true of the ingenious spectropolarimetric work of Centeno & Socas-Navarro (2008) than of any other study based on [O I] 630 nm.

Here we accurately redetermine  $\epsilon_{\text{Ni}}$ , and discuss the impact of the new value upon abundances from [O I] 630 nm. We show that  $\epsilon_{\text{Ni}}$  is model-dependent, contradicting claims by Centeno & Socas-Navarro that their technique allows a model-independent analysis.

## 2. MODEL ATMOSPHERES AND OBSERVATIONAL DATA

We used the same 3D LTE model atmosphere and line formation code as in earlier papers (e.g. Asplund et al. 2000b, 2004), described by Asplund et al. (2000a). We performed comparative calculations with three 1D models: HM (Holweger & Müller 1974), MARCS (Gustafsson et al. 1975; Asplund et al. 1997) and 1DAV (a contraction of the 3D model into one dimension by averaging over surfaces of equal optical depth). Each 1D model included a microturbulent velocity  $\xi_t = 1 \text{ km s}^{-1}$ . We averaged simulated intensity profiles over the temporal and spatial extent of the model atmosphere, and compared results with the Fourier Transform Spectrograph (FTS) disk-center atlas of Brault & Neckel (1987, see also Neckel 1999). We removed the solar gravitational redshift of  $633 \text{ m s}^{-1}$ , and convolved simulated profiles with an instrumental sinc function of width  $\Delta\sigma = \frac{c}{R} = 0.857 \text{ km s}^{-1}$ , reflecting the FTS resolving power  $R = 350\,000$  (Neckel 1999). We obtained abundances with the 3D model from profile-fitting via a  $\chi^2$ -analysis, fitting local continua independently with nearby clear sections of the spectrum. For 1D models we used the equivalent widths of 3D profile fits.

## 3. ATOMIC DATA AND LINE SELECTION

Our adopted Ni I lines and atomic data are given in Table 1. The most accurate Ni I oscillator strengths come from the laboratory FTS branching fractions (BFs) of Wickliffe & Lawler (1997), put on an absolute scale with the time-resolved laser-induced fluorescence (TRLIF) lifetimes of Bergeson & Lawler (1993). A small number of high-quality *gf*-values are also available from Johansson et al. (2003), based upon FTS BFs and a single TRLIF lifetime. To obtain the best estimate of the solar nickel content, we only consider lines with oscillator strengths available from these sources.

Nickel has five stable isotopes:  $^{58}\text{Ni}$ ,  $^{60}\text{Ni}$ ,  $^{61}\text{Ni}$ ,  $^{62}\text{Ni}$  and

<sup>1</sup> Cosmology, Particle Astrophysics and String Theory, Department of Physics, Stockholm University, AlbaNova University Centre, SE-106 91 Stockholm, Sweden; pat@fysik.su.se

<sup>2</sup> Oskar Klein Centre for Cosmoparticle Physics

<sup>3</sup> Max Planck Institute for Astrophysics, Postfach 1317, D-85741 Garching b. München, Germany; asplund@mpa-garching.mpg.de

<sup>4</sup> Most results were obtained whilst these authors were at the Australian National University Research School of Astronomy and Astrophysics, Mt. Stromlo Observatory, Cotter Rd., Weston Creek, ACT 2611, Australia.

<sup>5</sup> Centre Spatial de Liège, Université de Liège, avenue Pré Aily, B-4031 Angleur-Liège, Belgium

<sup>6</sup> Institut d'Astrophysique et de Géophysique, Université de Liège, Allée du 6 août, 17, B5C, B-4000 Liège, Belgium

<sup>7</sup> Observatoire Royal de Belgique, avenue circulaire, 3, B-1180 Bruxelles, Belgium

TABLE 1  
LIST OF NEUTRAL NICKEL LINES

Atomic levels		Isotope	Wavelength (nm, air)	Ex. Pot. (eV)	log <i>g f</i>	<i>g f</i> ref.	log $\gamma_{\text{rad}}$	$\sigma$	$\alpha$	$W_{\lambda}$ (pm)	log $\epsilon_{\text{Ni}}$ (3D)	Weight		
Lower	Upper													
3d <sup>8</sup> ( <sup>3</sup> F)4s4p( <sup>3</sup> P)	<sup>5</sup> G <sub>4</sub>	3d <sup>9</sup> ( <sup>2</sup> D)4d	<sup>3</sup> G <sub>5</sub>	<sup>58</sup> Ni <sup>60</sup> Ni	4740.1658	3.480	-1.730	WL	7.899	844	0.281	1.60	6.18	1
3d <sup>9</sup> ( <sup>2</sup> D)4p	<sup>3</sup> P <sub>1</sub>	3d <sup>9</sup> ( <sup>2</sup> D)4d	<sup>3</sup> P <sub>0</sub>		4811.9772 4811.9926	3.658	-1.592 -2.006	J03	8.285	-	-	2.12	6.20	1
3d <sup>8</sup> ( <sup>3</sup> F)4s4p( <sup>3</sup> P)	<sup>5</sup> G <sub>2</sub>	3d <sup>8</sup> 4s( <sup>4</sup> F)5s	<sup>5</sup> F <sub>3</sub>	<sup>60</sup> Ni	4814.5979	3.597	-1.620	WL	8.053	743	0.236	1.58	6.17	1
3d <sup>8</sup> ( <sup>3</sup> F)4s4p( <sup>3</sup> P)	<sup>5</sup> G <sub>3</sub>	3d <sup>8</sup> 4s( <sup>4</sup> F)5s	<sup>5</sup> F <sub>4</sub>		4874.7929	3.543	-1.450	WL	8.039	-	-	2.35	6.15	1
3d <sup>8</sup> ( <sup>2</sup> D)4p	<sup>3</sup> D <sub>2</sub>	3d <sup>8</sup> 4s( <sup>4</sup> F)5s	<sup>5</sup> F <sub>2</sub>		4886.7108	3.706	-1.780	WL	8.211	-	-	0.90	6.13	1
3d <sup>8</sup> ( <sup>3</sup> F)4s4p( <sup>3</sup> P)	<sup>5</sup> G <sub>4</sub>	3d <sup>8</sup> 4s( <sup>4</sup> F)5s	<sup>5</sup> F <sub>5</sub>		4900.9708	3.480	-1.670	WL	8.062	693	0.238	1.79	6.17	1
3d <sup>8</sup> ( <sup>3</sup> F)4s4p( <sup>3</sup> P)	<sup>5</sup> F <sub>4</sub>	3d <sup>9</sup> ( <sup>2</sup> D)4d	<sup>3</sup> G <sub>4</sub>		4976.1348	3.606	-1.250	WL	7.962	843	0.282	2.86	6.13	2
3d <sup>8</sup> ( <sup>3</sup> F)4s4p( <sup>3</sup> P)	<sup>5</sup> F <sub>4</sub>	3d <sup>8</sup> 4s( <sup>4</sup> F)5s	<sup>5</sup> F <sub>5</sub>		5157.9805	3.606	-1.510	WL	8.093	691	0.236	1.86	6.13	3
3d <sup>8</sup> ( <sup>3</sup> F)4s4p( <sup>3</sup> P)	<sup>3</sup> G <sub>5</sub>	3d <sup>8</sup> 4s( <sup>4</sup> F)5s	<sup>5</sup> F <sub>4</sub>		5504.0945	3.834	-1.700	WL	8.063	713	0.240	0.97	6.18	1
3d <sup>8</sup> ( <sup>2</sup> D)4p	<sup>1</sup> F <sub>3</sub>	3d <sup>9</sup> ( <sup>2</sup> D)4d	<sup>3</sup> G <sub>4</sub>		5510.0092	3.847	-0.900	WL	8.215	-	-	3.76	6.17	2
3d <sup>8</sup> ( <sup>2</sup> D)4p	<sup>1</sup> F <sub>3</sub>	3d <sup>8</sup> 4s( <sup>4</sup> F)5s	<sup>5</sup> F <sub>4</sub>		5537.1054	3.847	-2.200	WL	8.280	695	0.216	0.31	6.16	3
3d <sup>8</sup> ( <sup>3</sup> F)4s4p( <sup>3</sup> P)	<sup>3</sup> G <sub>3</sub>	3d <sup>9</sup> ( <sup>2</sup> D)4d	<sup>3</sup> G <sub>4</sub>		<sup>60</sup> Ni <sup>58</sup> Ni	5749.2795 5749.3039	3.941	-2.526 -2.112	WL	7.944	832	0.284	0.44	6.17
3d <sup>8</sup> ( <sup>3</sup> F)4s4p( <sup>3</sup> P)	<sup>3</sup> F <sub>4</sub>	3d <sup>9</sup> ( <sup>2</sup> D)4d	<sup>3</sup> G <sub>5</sub>	<sup>60</sup> Ni <sup>58</sup> Ni	6176.7980 6176.8200	4.088	-0.816 -0.402	WL	8.162	826	0.284	6.54	6.17	2
3d <sup>8</sup> ( <sup>3</sup> F)4s4p( <sup>3</sup> P)	<sup>3</sup> F <sub>4</sub>	3d <sup>8</sup> 4s( <sup>4</sup> F)5s	<sup>5</sup> F <sub>4</sub>	<sup>60</sup> Ni <sup>58</sup> Ni	6204.6048	4.088	-1.100	WL	8.244	719	0.247	2.11	6.19	3
3d <sup>8</sup> ( <sup>3</sup> F)4s4p( <sup>3</sup> P)	<sup>3</sup> F <sub>3</sub>	3d <sup>9</sup> ( <sup>2</sup> D)4d	<sup>3</sup> G <sub>4</sub>		6223.9710 6223.9914	4.105	-1.466 -1.052	WL	8.322	827	0.283	2.79	6.17	3
3d <sup>8</sup> ( <sup>3</sup> F)4s4p( <sup>3</sup> P)	<sup>3</sup> D <sub>3</sub>	3d <sup>9</sup> ( <sup>2</sup> D)4d	<sup>3</sup> G <sub>4</sub>	<sup>60</sup> Ni <sup>58</sup> Ni	6378.2328 6378.2580	4.154	-1.386 -0.972	WL	8.317	825	0.283	3.20	6.20	3
3d <sup>8</sup> ( <sup>3</sup> F)4s4p( <sup>3</sup> P)	<sup>3</sup> D <sub>3</sub>	3d <sup>8</sup> 4s( <sup>4</sup> F)5s	<sup>5</sup> F <sub>4</sub>	<sup>60</sup> Ni <sup>58</sup> Ni	6414.5884	4.154	-1.180	WL	8.369	721	0.249	1.68	6.20	2

NOTE. — Wavelengths and excitation potentials are from Litzen et al. (1993), and radiative damping is from VALD (Kupka et al. 1999). Except in the case of 481.2 nm, for which the transition was taken from VALD, transitions are from Wickliffe & Lawler (1997). References for *gf*-values are WL: Wickliffe & Lawler (1997) and J03: Johansson et al. (2003). Collisional damping parameters  $\alpha$  and  $\sigma$  are courtesy of Paul Barklem (private communication, 1999; now in VALD, Barklem et al. 2000). Equivalent widths are from profile fits using the 3D model.

$^{64}\text{Ni}$ , present in the approximate ratio 74:28:1:4:1 in the Earth (Rosman & Taylor 1998). Isotopic splitting of optical lines is small, and dominated by  $^{58}\text{Ni}$  and  $^{60}\text{Ni}$ . Litzen et al. (1993) have obtained accurate laboratory FTS wavelengths for the isotopic components of many Ni I lines, which we include in Table 1 where applicable. We model such lines with two components, distributing the total oscillator strength according to the terrestrial  $^{58}\text{Ni}$ : $^{60}\text{Ni}$  ratio. We are confident that the available data sufficiently describe the isotopic broadening of solar lines, as laboratory FTS recordings are far better resolved than lines in the Sun. Isotopic structure has not been included in other determinations of the solar nickel abundance.

We gave weightings to lines from 1 to 3 according to their appearance in the solar spectrum. Along with 16 unblended weak lines, we include the somewhat stronger Ni I 617.7 nm ( $W_{\lambda} = 6.54$  pm) owing to its clean line profile and its accurate atomic data. This line should be less affected by the rigors of strong line formation than single-component lines of the same equivalent width, thanks to the desaturating effects of isotopic broadening. To be conservative, we give this line a weighting of 2. Our list has only two lines in common with Biémont et al. (1980), mainly due to the absence of accurate *gf*-values for the 10 other lines used by those authors.

We took wavelengths and excitation potentials from Litzen et al. (1993), and radiative damping data from VALD (Kupka et al. 1999). For most lines, we used collisional broadening parameters calculated for individual lines by Paul Barklem (private communication, 1999; now in VALD, Barklem et al. 2000). For the remainder we interpolated in the tables of Anstee & O’Mara (1995) and Barklem & O’Mara

(1997). Transitions are from Wickliffe & Lawler (1997), except for Ni I 481.2 nm, where the transition designation is from VALD. The ambiguity in the identification of the upper level of this line (Johansson et al. 2003) has no impact, as apart from the slightly stronger 617.7 nm line, all our lines are quite insensitive to the adopted collisional broadening.

The paucity of good lines and atomic data in the optical makes an analysis of Ni II in the Sun rather difficult. We used 340.2 nm, 342.1 nm, 345.4 nm and 376.9 nm with Unsöld broadening enhanced by a factor of 2.0, obtaining wavelengths, transitions, radiative damping and excitation potentials from VALD. We compared results obtained with *gf*-values from two different theoretical sources (Fritzsche et al. 2000; Kurucz, <http://kurucz.harvard.edu/atoms.html>).

#### 4. NICKEL RESULTS

The mean nickel abundances we found using different model atmospheres are given in Table 2. Examples of profile fits to Ni I lines with the 3D model are given in Fig. 1, exhibiting similarly impressive agreement with observation as seen with other species (e.g. Asplund et al. 2000a, 2004). None of the models show abundance trends with equivalent width (Fig. 2), excitation potential nor wavelength, and the scatter is universally low, boding well for the internal consistency of all models. Very little difference exists between 3D and 1DAV abundances, implying that the mean temperature structure rather than atmospheric inhomogeneities is the main reason for the difference between the 3D and HM results. The 3D  $\epsilon_{\text{Ni}}$  is in excellent agreement with the meteoritic value (AGS05), whereas the HM value is not.

TABLE 2  
LOGARITHMIC SOLAR NICKEL ABUNDANCES (MEAN  $\pm$  1 STANDARD DEVIATION)

	3D	1DAV	HM	MARCS	Meteoritic
$\log \epsilon_{\text{Ni}}$ (Ni I lines)	$6.17 \pm 0.02$	$6.17 \pm 0.02$	$6.26 \pm 0.02$	$6.16 \pm 0.02$	$6.19 \pm 0.03$

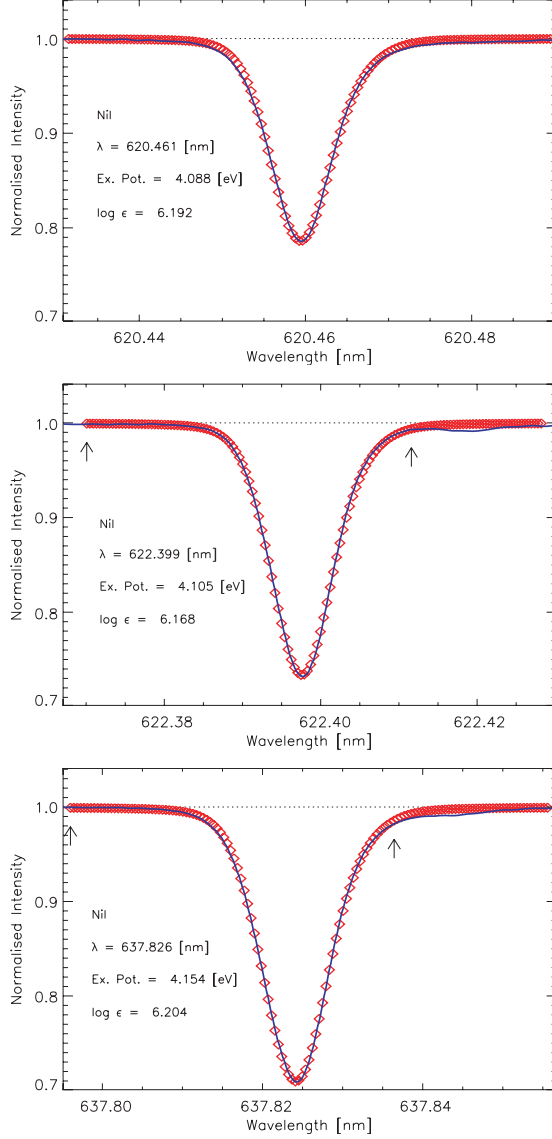


FIG. 1.— Example spatially- and temporally-averaged, disk-center synthesized Ni I line profiles (diamonds), compared with observed FTS profiles (solid lines). We removed the solar gravitational redshift from the FTS spectrum, convolved synthesized profiles with instrumental sinc functions and fitted them in abundance and line shift. Arrows indicate the windows used for profile fits; in the uppermost panel, we used the entire synthesized region.

Ni II lines give widely varying abundances, but the mean results are consistent with Ni I:  $\log \epsilon_{\text{Ni}} = 6.24 \pm 0.18$  with the 3D model and Fritzsche et al. (2000)  $gf$ -values, and  $\log \epsilon_{\text{Ni}} = 6.31 \pm 0.20$  with Kurucz values. All four lines are blended in the Sun, so the abundance scatter no doubt reflects both the  $gf$  uncertainties and the spectral crowding in the near-UV.

Given the large uncertainty in the Ni II result, we adopt the 3D Ni I result as the best estimate of the solar abundance:

$$\epsilon_{\text{Ni}} = 6.17 \pm 0.05.$$

The error is the sum in quadrature of the line-to-line scat-

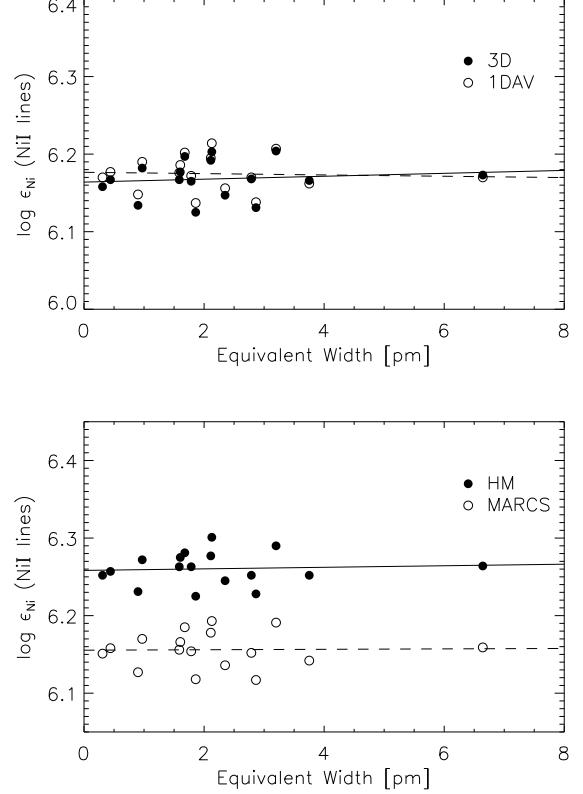


FIG. 2.— Solar nickel abundances indicated by Ni I lines, as computed with different model atmospheres. No substantial trends with line strength are visible with any of the four models. The similarity between 3D and 1DAV abundances suggests that the mean temperature structure of the 3D model is predominantly responsible for the difference between HM and 3D results, rather than the presence of temperature inhomogeneities.

ter ( $\pm 0.02$  dex) and possible systematics from the model atmosphere ( $\approx 0.05$  dex). AGS05 gave  $\epsilon_{\text{Ni}} = 6.23 \pm 0.04$ , from Reddy et al. (2003) using an ATLAS9 model (Kurucz, <http://kurucz.harvard.edu/grids.html>). Previous reviews (e.g. GS98) adopted  $6.25 \pm 0.09$ , by Biémont et al. (1980) using the HM model. Our value is 0.06–0.08 dex lower than earlier ones, and 0.09 dex less than our own best HM-based estimate. There is presently no evidence for non-LTE effects on our chosen lines in the Sun (Asplund 2005), but without a dedicated study we cannot rule them out. After adjusting for  $gf$ -values and equivalent widths, we find abundances 0.06 and 0.07 dex higher with the HM model than Biémont et al. for the two lines in common. We have not been able to trace the exact cause of these disparities, but tentatively attribute them to differences in radiative transfer codes, continuum opacities and implementations of the HM model.

#### 5. IMPLICATIONS FOR THE SOLAR OXYGEN ABUNDANCE

The revised solar nickel abundance presented here has a direct impact upon any derivation of the oxygen abundance using the [O I] 630 nm line, as this line is blended with one from Ni I (Allende Prieto et al. 2001).

Centeno & Socas-Navarro (2008) used the Stokes  $V$  profile of [O I] 630 nm to find an atomic ratio  $\epsilon_{\text{O,atomic}}/\epsilon_{\text{Ni}} = 210 \pm 24$  in a sunspot. They adopted an outdated  $gf$ -value for the [O I] 630 nm line (cf. Storey & Zeippen 2000), causing an overestimation of the ratio by 15% (+0.06 dex). They assumed  $\log \epsilon_{\text{Ni}} = 6.23$  to find  $\epsilon_{\text{O,atomic}}$  and converted this to a bulk  $\epsilon_{\text{O}}$  by calculating that 51% of oxygen resides in molecules. This is a reasonable assumption; in sunspots the only significant oxygen-bearing molecule is CO, which (roughly) forms as many molecules as there are carbon atoms available, due to the low temperatures. This number thus mirrors the assumed C/O ratio at the start of the calculation. That ratio only depends weakly on the choice of 3D or HM model, as seen in the shift from  $0.49 \pm 0.11$  to  $0.54 \pm 0.10$  between GS98 and AGS05. A more straightforward way of estimating the contribution from CO would be to say that the maximum  $\epsilon_{\text{CO}}$  is given by the adopted carbon abundance:  $\epsilon_{\text{O}} \approx \epsilon_{\text{O,atomic}} + \epsilon_{\text{C}}$ .

Centeno & Socas-Navarro claimed a model-independent analysis because neither their CO correction, nickel-to-atomic-oxygen ratio nor adopted  $\epsilon_{\text{Ni}}$  relied on an atmospheric model. Whilst the first statement is approximately true in the current debate, and the second is true of photospheric (but not sunspot) models, we have shown that  $\epsilon_{\text{Ni}}$  is not model-independent. The determination of  $\epsilon_{\text{O}}$  via this method is thus manifestly model-dependent, so there is no longer any reason to prefer placing a prior on the C/O ratio than on  $\epsilon_{\text{C}}$  directly. Using our new nickel abundance, correcting the [O I] 630 nm  $gf$ , adopting the  $\epsilon_{\text{C}}$  of AGS05 and fully propagating all errors, we find an oxygen abundance of  $\log \epsilon_{\text{O}} = 8.71 \pm 0.10$  instead of their  $8.86 \pm 0.07$ . Had we instead adopted the traditional sunspot model of Maltby et al. (1986) disfavored by Centeno & Socas-Navarro, we would have found  $8.67 \pm 0.10$ . Retaining Centeno & Socas-Navarro's prior on the C/O ratio (with the error thereupon given by AGS05), one would obtain  $8.74 \pm 0.10$  with their sunspot model and  $8.66 \pm 0.10$  with the Maltby et al. model. Clearly their method is not as model-independent as Centeno & Socas-Navarro argued.

Our new Ni abundance also modifies analyses of [O I] 630 nm in the quiet solar spectrum. Allende Prieto et al.

(2001), Asplund et al. (2004) and Ayres (2008) all allowed the Ni contribution to vary freely in their 3D profile-fitting of the 630 nm feature, whilst Caffau et al. (2008) fixed it with the Ni abundance of GS98. With the Ni abundances from Table 2 and the laboratory  $gf$ -value of the Ni I blend (Johansson et al. 2003), we can now accurately predict the Ni contribution to [O I] 630 nm. Independent of the adopted 1D or 3D model atmosphere, it is 0.17 pm in disk-center intensity, and 0.19 pm in flux. In terms of oxygen abundance, this implies a decrease by 0.04 dex to  $\log \epsilon_{\text{O}} \approx 8.65$  for the analysis of Asplund et al. (2004), further improving the excellent agreement between different indicators. The derived abundance of Ayres (2008) would decrease to  $\approx 8.77$  while that of Caffau et al. (2008) would increase to  $\approx 8.72$ . Because we now know the strength of the Ni blend, it is surprising that these two studies yield different results for the remaining contribution from oxygen, as they both rely on the same 3D CO<sup>5</sup>BOLD model. Since Caffau et al. employed several 3D snapshots whereas Ayres used only one, we tentatively consider the former more reliable. No Ni abundance has yet been produced with the CO<sup>5</sup>BOLD model, but regardless of its value our conclusions about the strength of the Ni I 630 nm blend, and thus its impact on oxygen abundances found by different authors, would remain unchanged. The difference of 0.07 dex in the revised Asplund et al. (2004) and Caffau et al. (2008) abundances from [O I] 630 nm probably reflects the different mean temperature stratifications of the two 3D models.

Given our reappraisal of the oxygen abundances of Centeno & Socas-Navarro (2008), Asplund et al. (2004) and Caffau et al. (2008), together with the recent study of Meléndez & Asplund (2008) using the [O I] 557.7 nm line, it now seems that results from forbidden oxygen lines are beginning to converge around  $\log \epsilon_{\text{O}} = 8.7$ .

We would like to take this opportunity to commemorate the work and life of Sverneric Johansson, his contribution to atomic spectroscopy in general and to nickel and [O I] 630 nm in particular. PS thanks IAU Commission 46, the ANU and the Australian Research Council for financial support.

#### REFERENCES

- Allende Prieto, C., Lambert, D. L., & Asplund, M. 2001, *ApJ*, 556, L63  
 Anders, E., & Grevesse, N. 1989, *Geochim. Cosmochim. Acta*, 53, 197  
 Anstee, S. D., & O'Mara, B. J. 1995, *MNRAS*, 276, 859  
 Asplund, M. 2005, *ARA&A*, 43, 481  
 Asplund, M., Grevesse, N., & Sauval, A. J. 2005, in *ASP Conf. Ser.* 336, ed. T. G. Barnes III & F. N. Bash (Astron. Soc. Pac., San Francisco), 25, (AGS05)  
 Asplund, M., Grevesse, N., Sauval, A. J., Allende Prieto, C., & Kiselman, D. 2004, *A&A*, 417, 751  
 Asplund, M., Gustafsson, B., Kiselman, D., & Eriksson, K. 1997, *A&A*, 318, 521  
 Asplund, M., Nordlund, Å., Trampedach, R., Allende Prieto, C., & Stein, R. F. 2000a, *A&A*, 359, 729  
 Asplund, M., Nordlund, Å., Trampedach, R., & Stein, R. F. 2000b, *A&A*, 359, 743  
 Ayres, T. R. 2008, *ApJ*, 686, 731  
 Ayres, T. R., Plymate, C., & Keller, C. U. 2006, *ApJS*, 165, 618  
 Barklem, P. S., & O'Mara, B. J. 1997, *MNRAS*, 290, 102  
 Barklem, P. S., Piskunov, N., & O'Mara, B. J. 2000, *A&AS*, 142, 467  
 Basu, S., & Antia, H. M. 2008, *Phys. Rep.*, 457, 217  
 Bergeson, S. D., & Lawler, J. E. 1993, *J. Opt. Soc. Amer. B*, 10, 794  
 Biémont, E., Grevesse, N., Huber, M. C. E., & Sandeman, R. J. 1980, *A&A*, 87, 242  
 Brault, J., & Neckel, H. 1987, *Spectral atlas of solar absolute disk-averaged and disk-centre intensity from 3290 to 12510 Å* (<ftp://ftp.hs.uni-hamburg.de/pub/outgoing/FTS-Atlas>)  
 Caffau, E., Ludwig, H.-G., Steffen, M., Ayres, T. R., Bonifacio, P., Cayrel, R., Freytag, B., & Plez, B. 2008, *A&A*, 488, 1031  
 Centeno, R., & Socas-Navarro, H. 2008, *ApJ*, 682, L61  
 Fritzsche, S., Dong, C. Z., & Gaigalas, G. 2000, *Atom. Data Nuc. Data Tables*, 76, 155  
 Grevesse, N., & Sauval, A. J. 1998, *Space Sci. Rev.*, 85, 161, (GS98)  
 Gustafsson, B., Bell, R., Eriksson, K., & Nordlund, Å. 1975, *A&A*, 42, 407  
 Holweger, H., & Müller, E. A. 1974, *Sol. Phys.*, 39, 19  
 Johansson, S., Litzén, U., Lundberg, H., & Zhang, Z. 2003, *ApJ*, 584, L107  
 Koesterke, L., Allende Prieto, C., & Lambert, D. L. 2008, *ApJ*, 680, 764  
 Kupka, F., Piskunov, N., Ryabchikova, T. A., Stempels, H. C., & Weiss, W. W. 1999, *A&AS*, 138, 119  
 Litzén, U., Brault, J. W., & Thorne, A. P. 1993, *Phys. Scr.*, 47, 628  
 Maltby, P., Avrett, E. H., Carlsson, M., Kjeldseth-Moe, O., Kurucz, R. L., & Loeser, R. 1986, *ApJ*, 306, 284  
 Meléndez, J., & Asplund, M. 2008, *A&A*, 490, 817  
 Neckel, H. 1999, *Sol. Phys.*, 184, 421  
 Reddy, B. E., Tomkin, J., Lambert, D. L., & Allende Prieto, C. 2003, *MNRAS*, 340, 304  
 Rosman, K. J. R., & Taylor, P. D. P. 1998, *Pure & Appl. Chem.*, 70, 217  
 Scott, P. C., Asplund, M., Grevesse, N., & Sauval, A. J. 2006, *A&A*, 456, 675  
 Socas-Navarro, H., & Norton, A. A. 2007, *ApJ*, 660, L153  
 Storey, P. J., & Zeippen, C. J. 2000, *MNRAS*, 312, 813  
 Unsöld, A. 1955, *Physik der Sternatmosphären*, MIT besonderer Berücksichtigung der Sonne., 2nd edn. (Springer, Berlin)  
 Wickliffe, M. E., & Lawler, J. E. 1997, *ApJS*, 110, 163